www.czasopisma.pan.pl PAN POLSKA AKADEMIA NAUK www.journals.pan.pl

Arch. Metall. Mater. **67** (2022), 2, 645-652

DOI: https://doi.org/10.24425/amm.2022.137801

E.R. MOLDOVAN[1], C. CONCHESO DORIA[2], J.L. OCAÑA MORENO[3], L.S. BALTES[1], E.M. STANCIU[1], C. CROITORU[1], A. PASCU[1], M.H. TIEREAN[1*]

GEOMETRY CHARACTERIZATION OF AISI 430 STAINLESS STEEL MICROSTRUCTURING USING LASER

Laser-generated surface patterns provide the means for local mechanical interlocking between the joined materials, tunes the wettability of surfaces that come in contact, and generally are the main factor for bonding strength enhancement, especially between dissimilar materials. This paper presents the influence of different patterning overlays generated with a pulsed laser on the surface of stainless-steel sheets. For all experiments, an overlapping degree of 90% has been chosen between three different patterns, while the engraving speed, pulse frequency and number of passes have varied. The textured surfaces' morphology was assessed through optical microscopy, and the roughness of the surfaces was correlated with the corresponding experimental parameters. The results have indicated promising insights for joining stainless steel to plastic materials, which is otherwise difficult to assess through usual welding techniques.

Keywords: microstructuring; laser; ferritic stainless steel; surface patterning

1. Introduction

Direct laser surface texturing (DLST) is a method that allows the surface improvement of an engineered material in terms of performance, for task-specific applications. It is a cutting-edge technique, having the advantage of obtaining surface features in micro and nano sizes, precise and reproducible textures, both on hard and brittle components. It is possible to be implemented on different categories of materials, such as metallic (stainless steel, titanium and its alloys, cobalt-chromium alloys, magnesium alloys, aluminum and alloys, copper, etc.), plastic (PP, PE, PEEK, PMMA, PLLA, etc.), ceramic (Al_2O_3, ZrO_2, etc.) and composite (glass fiber reinforced PP/aluminum, magnesium alloy/PET, AISI 304/PA6, C/SiC, SiC/SiC, etc). Usually, the pattern can be regular or irregular, in the form of grooves, dimples, bumps or other models. DLST is applied on joining of dissimilar materials [1,2], biomedical devices [3-9], tribological improvements [10-12], heat exchangers [13], surfaces wetting [14], photovoltaics industry [15,16], semiconductors patterning [17], painting [18].

The last five years have shown an increased research interest in the DLST technique [19,20]. To obtain the desired texture on the surface of material and at the same time to reduce the possible defects, it is of upmost importance to consider the following parameters: laser wavelength, intensity, energy per pulse, frequency of the laser pulses, the angle of incidence, number of cycles, polarization, repetition number and rate, scanning speed, focal distance, pulse overlapping, number of overlapped scanning layers [20].

Czotscher et al. [21] investigated 0.2 mm Al sheets with an YLP-HP laser (1065 nm laser beam) considering pulse duration 120 ns, power average 20…45 W, pulse energy 0.6…1 mJ, scanning speed 1m/s, repetition rate 20…60 KHz. The hole depth increases constantly after each pulse, also the hole diameter. A positive influence for lower pulse overlaps and smaller distances between the scanning lines were observed, that lead to a better mesh structure. Salstela et al. [22] studied the adhesion improvement of 5754-aluminum alloy substrate with epoxy resin. On the aluminum substrate, three different types of micro patterns were applied: microstructuring with micro-meshes, hierarchical sandblasting + micro-mesh printing and hierarchical micro-mesh printing + sandblasting. The objective was achieved by increasing the surface area with the number of locking points in substrate material; the hierarchical microstruc-

[1] TRANSILVANIA UNIVERSITY OF BRASOV, BRASOV, ROMANIA
[2] BSH ELECTRODOMÉSTICOS ESPAÑA S.A., ZARAGOZA, SPAIN
[3] UNIVERSIDAD POLITECNICA DE MADRID, MADRID, SPAIN

* Corresponding author: mtierean@unitbv.ro

turing providing the best solution. The condition is that mesh size should be large enough to allow filling with epoxy resin. Rauh et al. [23] analyzed the effect of micro-conically structured aluminum surface obtained by femtosecond laser ablation with 60 fs laser pulses in nitrogen atmosphere, and 6 ns laser pulses in an iodine/air atmosphere, by means of Nd:YAG laser with wavelength $\lambda = 1064$ nm, a maximal pulse energy of $E = 50$ mJ and $f = 20$ Hz pulse repetition rate. The best results concerning surface texturing was obtained in the case of femtosecond laser microstructuring, but iodine atmosphere also yielded satisfactory results. Knapp et al. [24] investigated three type of polymers: PP, PE and PEEK samples 30×70×8 (mm) in order to improve the adhesion with an Al-thin film. The laser source used in microstructuring the substrate had a wavelength of $\lambda = 355$ nm, a repetition rate of 10 kHz, a pulse duration of 33 ± 10 ns and a pulse energy of 10 W. The pattern type was 30×30 mm square grid with 0°/90° straight lines spaced by 50 µm or 200 µm. Experimental results showed that for PE and PEEK, laser texturing largely increases the adhesion if laser parameters are well adjusted. For PP, roughening of the surface seems to be more important. Mechanical adhesion mechanisms could also be optimized, being better controlled with precise and focalized laser ablation.

The improvement of PP tensile adhesive strength was studied by Matsuzaki et al. [25] through roll imprinting of undercut micropatterns on PP plates samples (30×20×1.5 mm). The undercut angle was found to be 25°, and the tensile adhesive strength was 1.7 times higher than that of the specimen without surface modification. The aim of Cardoso et al. [14] was to increase the hydrophobicity of polymeric poly(1-methoxy-4-(O-disperse Red 1)-2,5-bis(2-methoxyethyl) benzene) surface film through laser microstructuring with an Nd:YAG laser operating at 850 Hz repetition rate, 70…532 nm pulses, 17…65 nJ energy, and 1mm/s translation speed. Square-shaped-pillars morphologies with distinct periodicities, from 5.0 µm to 500 µm were applied. A roughness increasing from Ra = 100 nm to Ra = 450 nm was observed, from non microstructured to microstructured samples. These results permited the fabrication of surfaces with contact angle higher than 150°.

Hybrid joints between dissimilar materials, such as metals and non-metals (polymers, ceramics) [26] represent a widely customizable approach used in automotive industry [2,27], industrial manufacturing [28,29], as well as in biomedical [30], packing [31], aerospace [32], and households [19] industries, aiming lightweight structures that are optimized in terms of production costs and strength [32-34]. Microstructuring can be used before joining dissimilar materials as pre-treatment in laser processing to achieve a better mechanical interlocking [28,31] and to control the physical, chemical and mechanical properties of hybrid joints [35].

The goal of this research paper is to study of the influence of different patterning overlays prepared by DLST with different processing parameters on the surface's geometry, having as potential application metal-to-polymer joining.

2. Experiment

2.1. Material

The proposed material for microstructuring is the ferritic stainless steel AISI 430 (ACX 500, EN 1.4016) provided by Acerinox SA, Madrid, Spain (TABLE 1, TABLE 2). The material is ductile and can be shaped using rolling, bending, and embossing. It has a quite good corrosion resistance to various saline or acidic environments. As the base alloy of the ferritic group, this grade 430 ferritic stainless steel is only readily available in sheet and coil (up to 1.2 mm thick) most commonly in BA (bright annealed) or 2B (moderately reflective) finishes. Samples were cut from a large sheet with 80 mm×25 mm×0.5 mm dimensions.

TABLE 1

Chemical composition according to EN 10088-2 and ASTM A-240

Element (%)	C	Si	Mn	P	S	Cr	N
Concentration	≤0.08	≤1.00	≤1.00	≤0.040	≤0.015	16.00-18.00	≤0.045

TABLE 2

Mechanical properties as per EN 10088-2 and ASTM A-240

Material	$Rp_{0.2}$ [MPa]	Rm [MPa]	ASO [%]	HRB
AISI 430	>260	450-600	>20	<185

2.2. Design of AISI 430 samples

For this study three design patterns were used, presented in Fig. 1. The surface of microstructured area is 20×19.5 mm (design type A), 18×16 mm (design type B) and 19.5×17 mm (design type C).

2.3. Microstructuring of AISI 430 ferritic stainless steel

The microstructuring has been performed with an infrared Nd Fiber Diode-Pumped TruMark 5020 laser made by Trumpf. The equipment has an average power of 20 W, wavelength of 1062 nm, pulse frequency from 5 to 1000 kHz, integrated with a highly dynamic scanner module. The experiments have been carried out using a standard design of experiments, in which a parameter was kept constant, while the others were varied. The constant parameters were: the pulsed peak power of 3.8 kW at 20 kHz, number of impulses per point (1), defocus 0 mm, 100 µm diameter spot, and a focal distance of 254 mm. An angle alignment of 3 degrees of the laser beam axis with the perpendicular to the sample surface was adopted, to prevent damaging the laser optical fiber due to specular reflection on the surface of the samples. Variable parameters are the frequency (30÷100 kHz), speed (300÷1000 mm/s) and number of passes-repetition (1÷20). Fig. 2 shows the variation of the pulse duration as a function

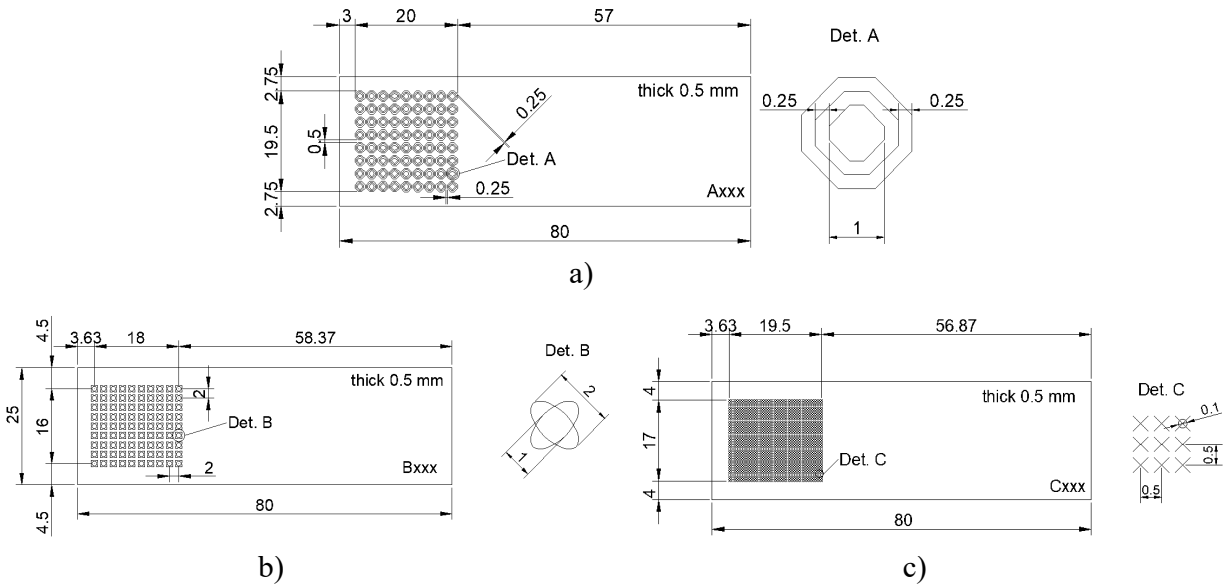

Fig. 1. Sample types: (a) design A, hexagonal shape 2×2 mm (center to center), (b) design B, elliptical shape 2×2 mm (center to center), (c) design C, circle diameter ϕ0.1 mm

of speed. Before applying the microstructuring process, the samples were cleaned with isopropanol for cleaning and degreasing the samples. All the microstructured samples were encoded depending on the speed, frequency and the number of repetitions. A minimum overlapping (O_v) ≥ 90% of the successive laser spots was considered for the beam integrity. From the obtained samples, only representative ones have been chosen and discussed.

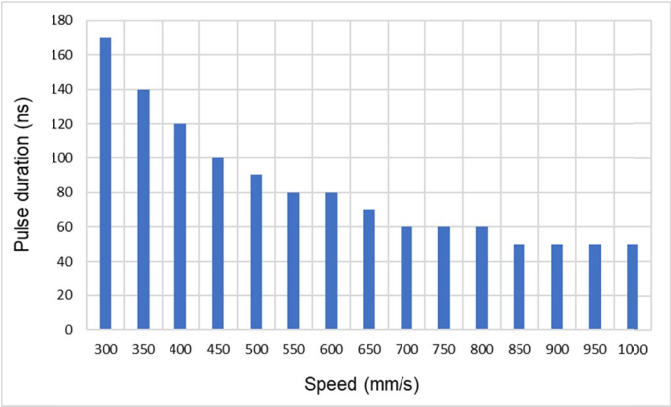

Fig. 2. Pulse duration correlation with the scanning speed during microstructuring

2.4. Materials characterization

All the optical micrographs were acquired with an Olympus BX35 upright optical microscope and the images have been captured using the Olympus DP73 camera with an Olympus TH4 halogen lamp power supply unit for brightness control and plan phase contrast objectives (UPLFLN-PH series). The 3D images display and measurement have been acquired with Olympus Image Analysis software using the surface view feature (thickness of the layer on the height was set for 1 µm in automatic processes). For measuring the roughness of the microstructured surface a roughness tester ISR-100 was used, with a traverse speed of 5 mm/s, measuring force 4 mN, and accuracy ±10%.

3. Results and discussion

The microstructuring is performed due to the laser beam local ablation of the material, generating grooves with a certain depth and width, as a function of the operational parameters. Also, a part of the ablated material can be deposited near the groove as recast material dimples (Fig. 3). Amend et al. [29] highlighted that the groove width (linear distance of the cavity, measured between the redeposited material dimples) has a significant influence on the surface properties of the material. Also, Rodríguez-Vidal et al. point out that tensile-shear mechanical performance is the changing factor as represented by geometry and cavity aspect ratio [33].

The cross-section optical micrographs of sample A (speed 300 mm/s, frequency 30 kHz, pulse duration 170 ns) are presented in Fig. 4. The 3D optical microscopy maps of sample

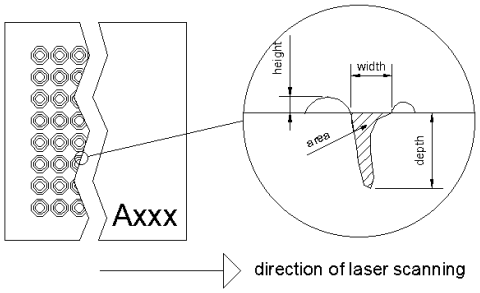

Fig. 3. Geometry characterization (height, width and area) of microstructuring on AISI 430

A (speed 300 mm/s, frequency 30 kHz, pulse duration 170 ns) are presented in Fig. 5. The optical micrographs were used to measure the depth and width of the grove, as well as the recast material deposited on/near the groove edges (Fig. 6).

According to Fig. 6, the area and depth of the microstructure increases until 13 repetitions of microstructuring. With the increase in repetition, the recast material elevation increases as well. Also, inversely proportional to the number of repetitions,

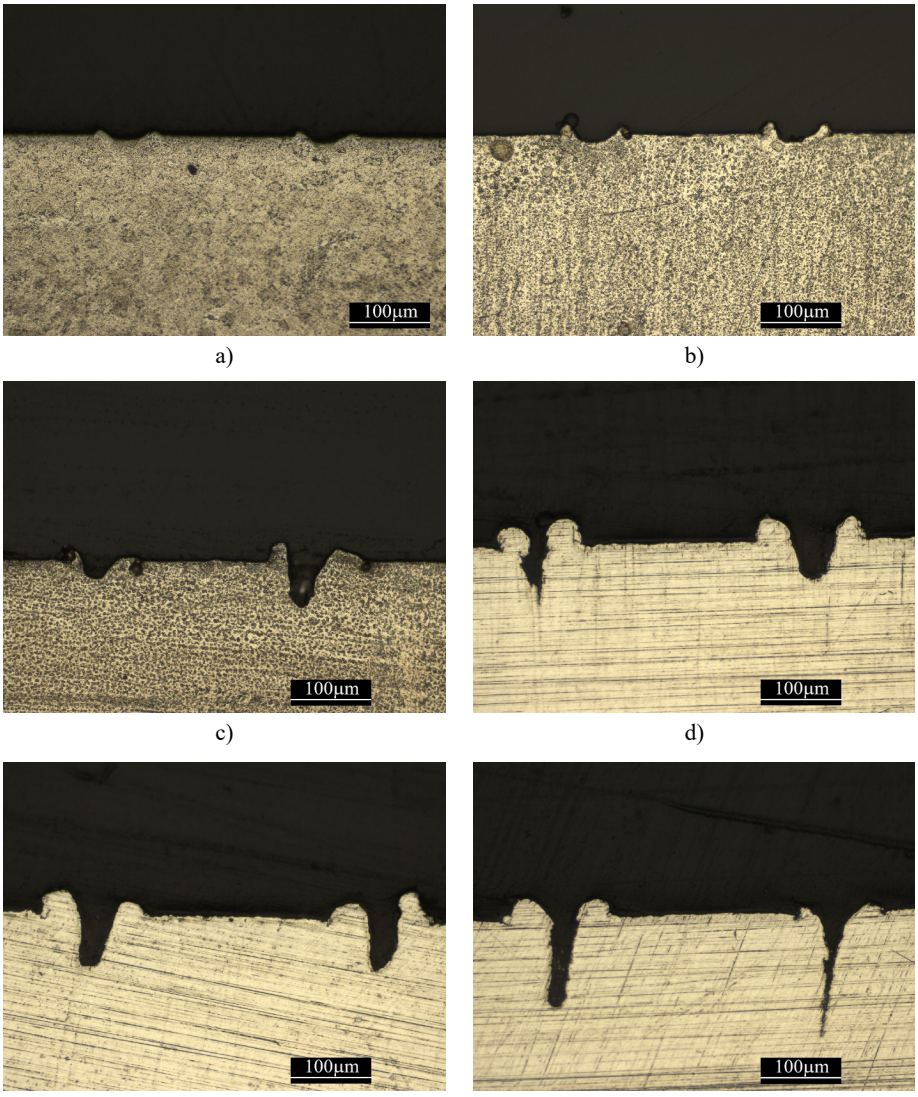

Fig. 4. Cross section views of microstructured AISI 430 stainless steel, design type A, speed 300 [mm/s], frequency 30 [kHz] and number of repetitions 2 (a), 5 (b), 7 (c), 10 (d), 13 (e), 17 (f)

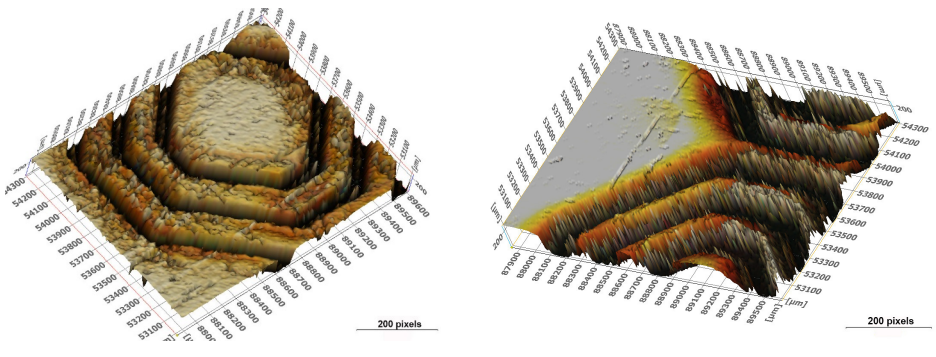

Fig. 5. 3D images of microstructured AISI 430 stainless steel, design type A, speed 300 [mm/s], frequency 30 [kHz] and number of repetitions 2 (a) and 17 (b)

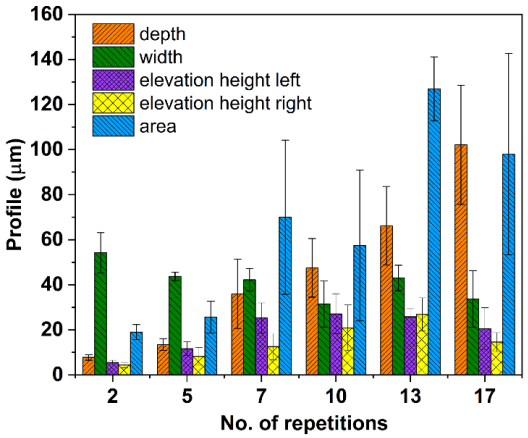

Fig. 6. Variation of the microgrooves' dimensions of microstructured stainless steel AISI 430 for design type A

the width of the groove tends to decrease. This tendency occurs because in the case of increased repetition the expelled material can no longer reach the surface of the workpiece as recast material, and instead will be deposited on the walls of the hollow narrowing the width of the groove. The deposited recast material is influenced by the laser beam angle alignment, resulting in one part of the recast material to be larger than the other side, depending on the laser beam direction.

The difference is visible when it comes to the number of repetitions in the case of laser passing and in the increasing of speed. At low speed and a maximum number of repetitions, it can be observed that groove material is mainly expulsed as recast material, and the micro-grooves have the pulsed beam laser shape. At lower number of repetitions, a small deformation of the stainless steel can be noted. In the case of type B design

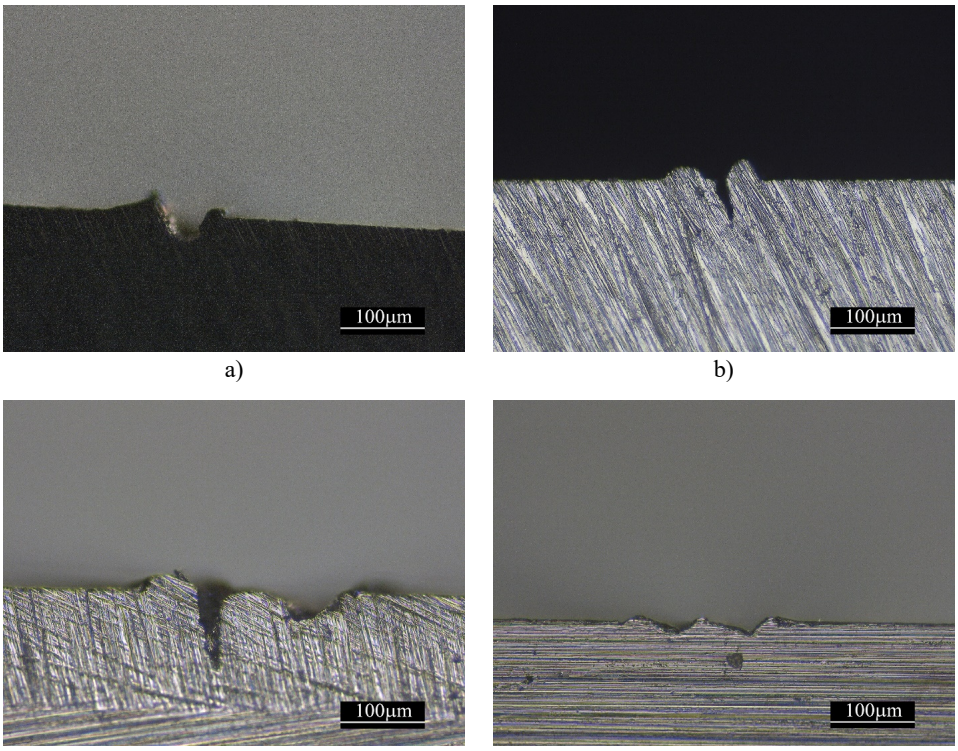

a) b) c) d)

Fig. 7. Cross section views of microstructured AISI 430 stainless steel, design type B, frequency 30 [kHz], speed 300 [mm/s], number of repetitions 10 (a); 20 (b); frequency 40 [kHz], speed 400 [mm/s], number of repetitions 20 (c); frequency 50 [kHz], speed 500 [mm/s], number of repetitions 10 (d)

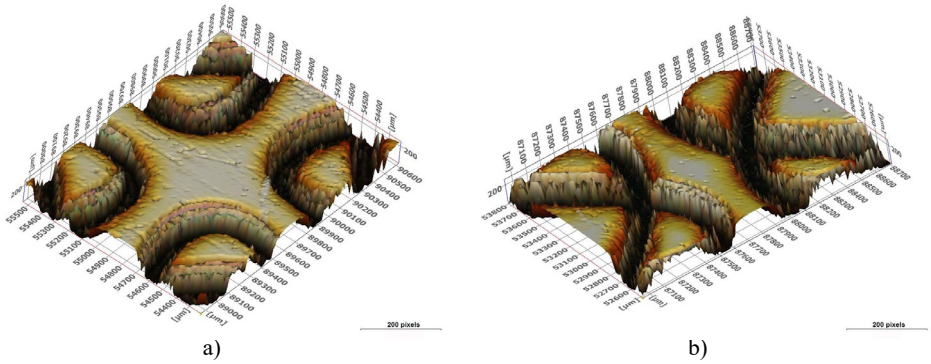

a) b)

Fig. 8. 3D images of microstructure frequency 30 [kHz], speed 300 [mm/s], number of repetitions 10 (a) and 20 (b)

(Fig. 7 and Fig. 8), the grooves are wider and shallower than for the other two designs. This is a consequence of the expelled material that has been deposited inside the groove at a lower position than in design type A.

In Fig. 9 the results indicate an increase in width with the scanning speed increasing, while the recast material elevation and area of depth displaying a relatively constant tendency.

In the case of design type C (Fig. 10) the lack of elevation of the recast material can be noticed. Due to this fact, the elevation's height is missing from Fig. 11. With the increase in speed, depth, width and area decreasing has been remarked.

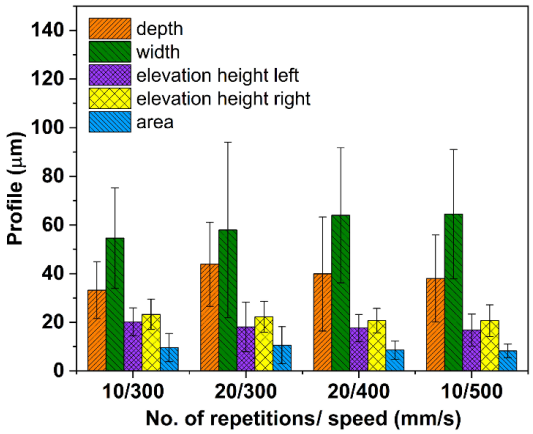

Fig. 9. Variation of the microgrooves' dimensions of microstructured stainless steel AISI 430 for design type B

Even if the same speed, frequency, and number of repetitions were used for designs A, B and C, the geometry of applied microstructure has an important role. From the cross-section optical micrographs (Figs. 4, 7 and 10) and profile histograms (Figs. 6, 9 and 11), it can be observed that the material displacement is less pronounced for design type B, comparing with designs type A and C. The same observation can be made in the case of design type C in comparison with design type B and A (after 13 no. of repetition of microstructuring operation) regarding the expulsed material.

The analyzed roughness parameters (Fig. 12) are Ra (the arithmetic average, the absolute values of the profile within base length), Rz (the height average, absolute values of heights of the top five prominences and of the bottom, or peak-to-valley heights) and Rt (total height of profile, from the lowest point to the highest peak).

Comparing the roughness after microstructuring with the roughness of the raw surface (Ra = 0.681 µm, Rz = 2.253 µm, Rt = 8.828 µm), it can be seen that design A possibly generates a better anchoring of the welded joints in terms of shear strength in the directions of the sheet surface.

4. Conclusions

The pulsed laser offers a fast, easy and clean operation in metal microstructuring. Microstructuring is essential in different

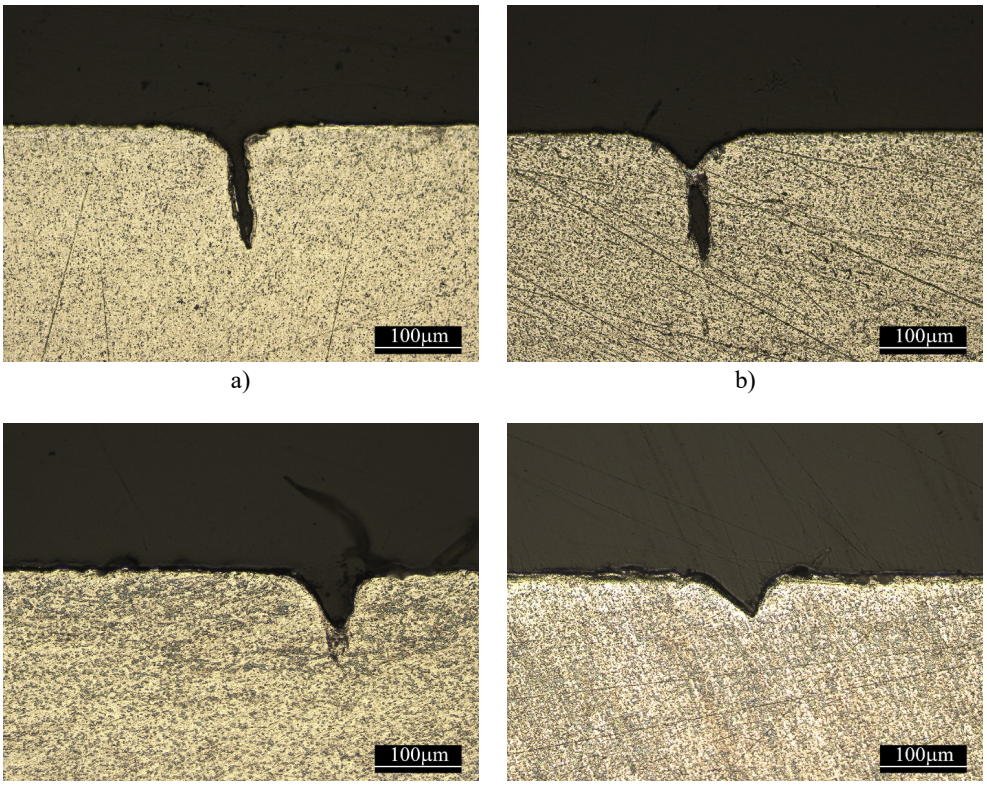

Fig. 10. Cross section views of microstructured AISI 430 stainless steel, design type C: frequency 30 [kHz], speed 300 [mm/s], number of repetitions 10 (a); 15 (b); frequency 50 [kHz], speed 500 [mm/s], and number of repetitions 15 (c); frequency 80 [kHz], speed 800 [mm/s], number of repetitions 15 (d)

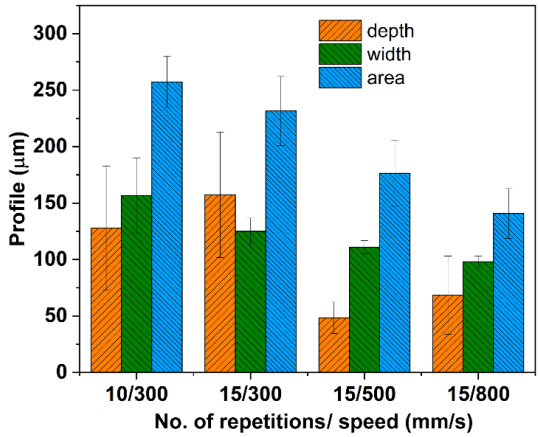

Fig. 11. Variation of the microgrooves' dimensions of microstructured stainless steel AISI 430 for design type C

application domains, ranging from biomaterials to hybrid joints between dissimilar materials, due to the formation and interlocking of grooves, which are cavities (in cross-section) ablated by the laser, a part of the ablated material being redeposited on the groove edges as small dimples. The results presented in the paper have indicated that the parameters of the laser micropatterning have a marked influence on the grove morphology, and consequently on the surface or joining properties of the materials.

From the three studied micropatterning designs, hexagonal, elliptical and circular, it has been observed that the hexagonal pattern generates the highest surface roughness (also the highest depth of the grooves), followed by the circular one, which could prove beneficial for joining operations. On the other hand, shallower and wider grooves (such as those obtained for the elliptical pattern) could provide a better crevice corrosion resistance for coated assemblies. Further studies will be performed on the characterization of the micropatterned materials surface properties and behavior in metal-plastic hybrid joints.

REFERENCES

[1] K. Shimamoto, Y. Sekiguchi, C. Sato, Int. J. Adhes. Adhes. **67**, 31-37 (2016).

[2] K. Vand der Straeten, I. Burkhardt, A. Olowinsky, A. Gillner, Physcs. Proc. **83**, 1137-1144 (2016).

[3] R.A. Delgado-Ruız, J.L. Calvo-Guirado, P. Moreno, J. Guardia, G. Gomez-Moreno, J.E. Mate-Sanchez, P. Ramirez-Fernandez, F. Chiva, J. Biomed. Mater. Res. B Appl. Biomater. **96** (1), 91-100 (2011).

[4] W. Liu, S. Liu, L. Wang, Coatings **9** (4), 249 (2019).

[5] M. de la Cruz Lorenzo, M. Portillo, A. Albaladejo, Photon Lasers Med. **1** (3), 171-182 (2012).

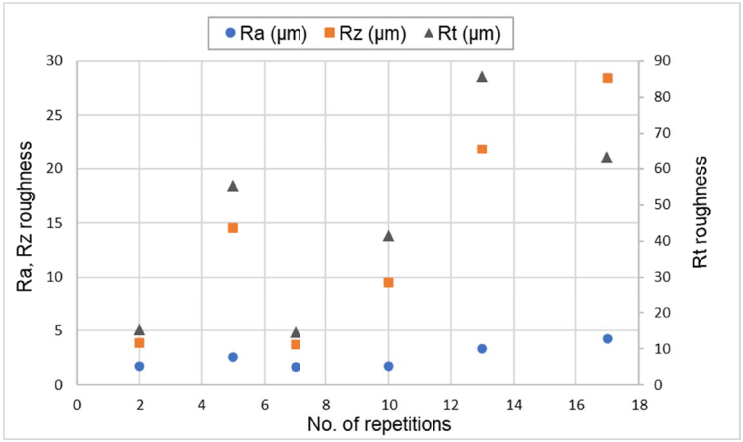

a)

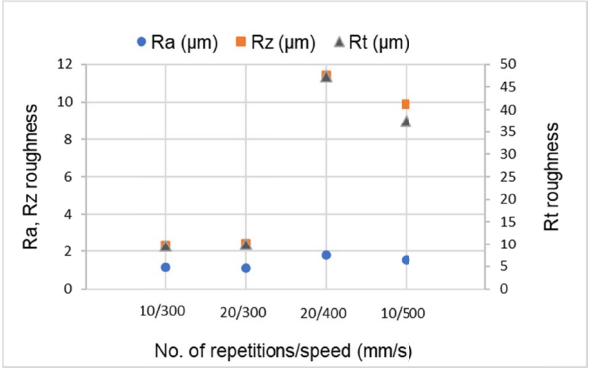

b)

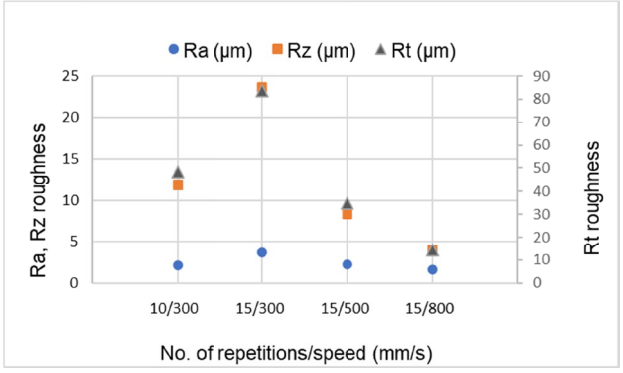

c)

Fig. 12. Roughness results on microstructured AISI 430 stainless steel: (a) design A, (b) design B, (c) design C

[6] G. Hu, K. Guan, L. Lu, J. Zhang, N. Lu, Y. Guan, Engineering **4** (6), 822-830 (2018).

[7] A. Carvalho, L. Grenho, M.H. Fernandes, A. Daskalova, A. Trifonov, I. Buchvarov, F.J. Monteiro, Ceram. Int. **46** (2), 1383-1389 (2020).

[8] R. Ortiz, I. Aurrekoetxea-Rodríguez, M. Rommel, I. Quintana, M. dM Vivanco, J.L. Toca-Herrera, Polymers **10** (12), 1337 (2018).

[9] N. Sirdeshmukh, G. Dongre, Mater. Today-Proc. **44**, 2348-2355 (2021).

[10] A.T.T. Nguyen, M. Brandt, A.C. Orifici, S. Feih, Int. J. Adhes. Adhes. **66**, 81-92 (2016).

[11] E. Rodriguez-Vidal, C. Sanz, J. Lambarri, J. Renard, V. Gantchenko, Physcs. Proc. **83**, 1110-1117 (2016).

[12] G. Dumitru, V. Romano, H.P. Weber, H. Haefke, Y. Gerbig, E. Pflüger, Appl. Phys. A **70**, 485-487 (2000).

[13] M. Adjim, R. Pillai, A. Bensaoula, D. Starikov, C. Boney, A. Saidane, J. Heat Transfer. **129** (7), 798-804 (2007).

[14] M.R. Cardoso, V. Tribuzi, D.T. Balogh, L. Misoguti, C.R. Mendonc, Appl. Surf. Sci. **257**, 3281-3284 (2011).

[15] S. Itapu, D.G. Georgiev, V. Devabhaktuni, J. Electromagnet. Wave, **29** (12), 1547-1556 (2015).

[16] J.E. Carey, PhD thesis, Femtosecond-laser Microstructuring of Silicon for Novel Optoelectronic Devices, Harvard University, Cambridge, Massachusetts, USA (2004).

[17] C. Samoila, D. Ursutiu, A. Tavkhelidze, L. Jangidze, Z. Taliashvili, G. Skhiladze, M. Tierean, Nanotechnology **31** (3), 035301 (2020).

[18] A. Guarnaccio, C. Belviso, P. Montano, F. Toschi, Sx. Orlando, G. Ciaccio, S. Ferreri, D. Trevisan, D. Mollica, G.P. Parisi, P. Dolce, A. Bellucci, A. De Stefanis, D.M. Trucchi, V. Valentini, A. Santagata, F. Cavalcante, A. Lettino, L. Medici, P.P. Ragone, V.G. Lambertini, Surf. Coat. Tech. **406**, 126727 (2021).

[19] E. Rodriguez-Vidal, C. Sanz, C. Soriano, J. Leunda, G. Verhaeghe, J. Mater. Process. Tech. **229**, 668-677 (2016).

[20] A. De Zanet, V. Casalegno, M. Salvo, Ceram. Int. **47**, 7307-7320 (2021).

[21] T. Czotscher, F. Vollertsen, Physcs. Proc. **83**, 53-61 (2016).

[22] J. Salstela, M. Suvanto, T.T. Pakkanen, Int. J. Adhes. Adhes. **66**, 128-137 (2016).

[23] S. Rauh, K. Wöbbeking, M. Li, W. Schade, E.G. Hübner, ChemPhysChem **21**, 1644-1652 (2020).

[24] W. Knapp, D. Djomani, J.F. Coulon, R. Grunchec, Physcs. Proc. **56**, 791-800 (2014).

[25] R. Matsuzaki, N. Tsukamoto, J. Taniguchi, Int. J. Adhes. Adhes. **68**, 124-132 (2016).

[26] E. Moldovan, M.H. Tierean, E.M. Stanciu, B. Transilvania Univ. **10** (1) 39-46 (2017).

[27] J.P. Bergmann, M. Stambke, Physcs. Proc. **39**, 84-91(2012).

[28] A. Cenigaonaindia, F. Liébana, A. Lamikiz, Z. Echegoyen, Physcs. Proc. **39**, 92-99 (2012).

[29] P. Amend, S. Pfindel, M. Schmidt, Physcs. Proc. **41**, 98-105 (2013).

[30] X. Wang, P. Li, Z. Xu, X. Song, H. Liu, J. Mater. Process. Tech. **210**, 1767-1771 (2010).

[31] A. Roesner, S. Scheik, A. Olowinsky, A. Gillner, U. Reisgen, M. Schleser, Physcs. Proc. **12**, 370-377 (2011).

[32] F.L. Palmieri, M.A. Belcher, C.J. Wohl, K.Y. Blohowiak, J.W. Connell, Int. J. Adhes. Adhes. **68**, 95-101 (2016).

[33] E. Rodriguez-Vidal, J. Lambarri, C. Soriano, C. Sanz, G. Verhaeghe, Physcs. Proc. **56**, 835-844 (2014).

[34] K. Schricker, M. Stambke, J.P. Bergmann, K. Bräutigam, P. Henckell, Physcs. Proc. **56**, 782-790 (2014).

[35] A.V. Brover, L.D. D'yachenko, Met. Sci. Heat Treat. **51** (5-6), 292-296 (2009).